FLOW CHARACTERIZATION AND MHD TESTS IN HIGH ENTHALPY ARGON FLOW

Lars Steffens [(1)], Uwe Koch [(1)], Burkard Esser [(1)], Ali Gülhan [(1)]

[(1)] German Aerospace Center (DLR), Linder Höhe 51147 Köln, Germany,
Email: lars.steffens@dlr.de, uwe.koch@dlr.de, burkard.esser@dlr.de, ali.guelhan@dlr.de

ABSTRACT

For recent argon based magnetohydrodynamic (MHD) experiments in the DLR arc heated facility L2K the free stream plasma has been characterized. Suitable states for MHD test have been identified by maximizing the free stream electron density. Argon flows have been used due to the reduced chemical complexity of the plasma. The characterization methods include microwave interferometry (MWI), Langmuir probe measurements, Pitot probe profiles and spectroscopic methods like diode laser absorption spectroscopy (DLAS) and emission spectroscopy.

The influence of a magnetic field on the heat transfer to the model has been studied with cylindrical stagnation point models, using both permanent and electromagnets with surface fields up to 0.54 T. To verify the influence of the field to the heat transfer both the shock distance and the surface heat flow have been observed.

1. INTRODUCTION

The use of magnetohydrodynamic effects has been proposed for several benefits concerning atmospheric re-entry including heat flux mitigation [1] and blackout mitigation [2]. Understanding of MHD needs elaborate numerical simulation tools as well as their experimental verification in ground based facilities. Modelling of MHD influenced weakly ionized hypersonic flows is difficult due to the complexity of the system [3]. The coupling between a magnetic field and plasma is given by the commonly anisotropic electric conductivity of the plasma, which strongly depends on the thermodynamic and chemical state of the plasma. Therefore a thorough characterization of the plasma flow in ground based facilities is an essential part of understanding the influences of MHD flows during re-entry and thus for designing MHD applications.

2. ARC HEATED FACILITY L2K

For the tests the L2K facility has been used. L2K is on eof the test legs of DLR's arc heated facility LBK. A sketch of LBK is given in Fig. 1. The principal component of L2K is a Huels-type arc heater that has a maximum electrical power of 1.4 MW allowing to achieve cold wall heat fluxes in air flow up to 4 MW/m^2 at stagnation pressures up to 250 hPa. Hypersonic free stream velocities are provided by a convergent-

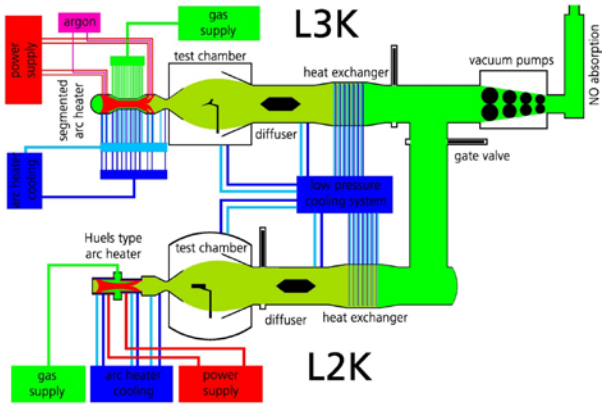

Figure 1. Arc heated facilities LBK of DLR.

divergent nozzle. The nozzle's expansion part is conical with a half angle of 12°. Different throat diameters from 14 mm to 29 mm are available and can be combined with nozzle exit diameters of 50 mm, 100 mm, 200 mm, and 300 mm. So, the facility setup can effectively be adapted to particular necessities of a certain test campaign. To fit the scale of the different used models, the 100 mm and the 200 mm nozzle exit diameter have been used for MHD test. A more detailed description of the facility is given by Gülhan et al. [4-6].

3. FLOW CHARACTERIZATION METHODS

Coriolis gas mass flow meter and reservoir pressure transducer have been used to continuously monitor the mass flow rate and the reservoir pressure during the tests. A Pitot probe has been used for determining the Pitot pressure profile across the flow. The Pitot pressure profiles are used to derive density and the beam width.
Emission spectroscopy with a Fourier transform infrared spectrometer (FT-IR) has been used to study the species spectra and the electronic excitation state of both the free stream and within the reservoir chamber of the arc heater. For a summary of emission spectroscopy results see [7,8]. Laser Induced Fluorescence Spectroscopy (LIF) on NO molecules has been used to determine the rotational temperature and concentration within the free stream and the bow shock layer [9,10].

DLAS on CO molecules has been used to determine the heavy particle translational temperature as well the flow velocity of the free stream.

MWI has been used for line-of-sight determination of the electron density as well as determining the flow velocity. Different types of electrostatic probes have been used to estimate the electron temperature.

Transmission spectra of microwaves have been used to determine the plasma frequency and thus the maximum electron density of the free stream.

3.1. Diode Laser Absorption Spectroscopy

DLAS was applied on carbon monoxide (CO) molecules for measuring the flow velocity and the translational temperature using a diode laser emitting in the wavelength range from 2330 to 2335 nm at room temperature. DLAS is a line-of-sight method and the interpretation of the measurements has to take into account the homogeneity of the flow field. The velocity of the gas molecules is proportional to the spectral shift of the absorption signal and the translational temperature is determined from the half width of the absorption profile. In order to provide the required carbon monoxide for DLAS measurements, the argon flow was seeded with 20% of carbon dioxide which partially dissociates to carbon monoxide at high temperatures.

The measured velocity did not change significantly when the amount of seeding was changed from 5% to 40%. For the measurement conditions in L2K, the divergence of the flow direction tends to increase the extracted velocity value while shear layer effects in the outer region of the free stream tend to decrease it. Concerning the temperature measurement the broadening of the signal due to the shear layer leads to increased temperature values. As no quantitative information about the divergence of the flow vectors and the thickness of the shear layer is available, the presented data should be used for a qualitative interpretation of the flow properties [10].

3.2. Microwave Interferometry

MWI is used for measuring the electron density and the flow velocity of the free stream. A MWI 2650 microwave interferometer measures the phase shift of microwaves passing the plasma. Electrons in the measurement volume reduce the permittivity and thus the optical path length on the way through the plasma. Thus the phase shift is directly linked to the average line of sight electron density in the measurement volume between emitter and detector. The geometrical path length is determined by the Pitot probe profiles. During this test campaign the flow velocity was also measured using two coupled microwave interferometer setups, MWI 2650 and MWI 2650-V. The MWI 2650 is placed in 230 mm distance from the nozzle exit, the MWI 2650-V in 430 mm distance. Fluctuations in the electron density measurements of the two devices were correlated with time and by knowing the distance between the two measurement volumes the flow velocity could be evaluated. In contrast to the above described DLAS technique no seeding of the flow is required.

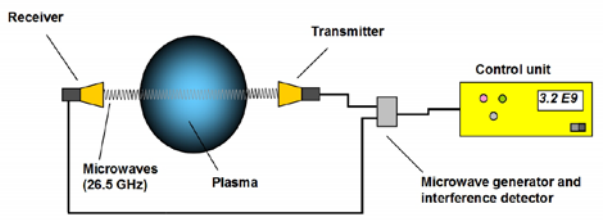

Figure 2. Scheme of microwave interferometer setup.

The experimental setup of the MWI 2650 is sketched in Fig. 2. The measured electron densities and flow velocities are listed in Tab. 1, 2 and 4 for all flow states.

3.3. Electrostatic probes

Langmuir probes in single [11], double [12] and triple configuration [13] were used to determine the electron density as well as the electron temperature. To exclude shock effects between the wires the probe is placed behind the bow shock in the stagnation point region of a stagnation point model of 70 mm diameter. A picture of the Langmuir triple probe setup in Argon flow is given in Fig. 3. In this picture the bow shock in front of the triple wire arrangement is clearly visible. The electron temperature is supposed to be effected only by a small amount by the shock due to the higher speed of sound of the electron gas, so that the free stream electron temperature can be approximated by the measured value. During the single and double probe measurements the probes was placed on the flow axis. With the triple probe also density profiles across the flow have been recorded.

3.4. Microwave Plasma Transmission Spectroscopy (MPTS)

Plasma is highly absorptive for electromagnetic waves at wavelength below the plasma frequency. By recording microwave spectra in the vicinity of the plasma frequency it is possible to determine the plasma frequency as well as getting an estimate for the maximum electron density in the transmission volume. Microwave spectra from 1 GHz to 11 GHz are transmitted through the Argon flow with a set of two left circular polarized antennas, connected to a spectrum analyser with tracking generator recording the spectra. A sketch of the setup is given in Fig. 4.

Circular polarization has been chosen to minimize interference effects in the chamber due to reflections at the metallic test chamber wall. About 40 spectral traces were taken within about 20 s. The spectra are processed

by taking the moving average of every trace with a width of 800 MHz to remove remaining interference and noise influence. Then the average over all traces of one experimental run is taken and the resulting signals with and without flow are subtracted from each other to get the attenuation signal.

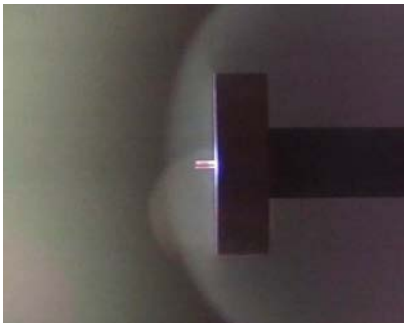

Figure 3. Langmuir triple probe in Argon flow.

Resulting attenuation curves for different 200 mm nozzle exit diameter states are shown in Fig. 6. The different states show clearly distinct attenuation curves. For each curve he attenuation drops to almost zero above the maximum plasma frequency f_p.

The maximum plasma frequency f_p of the flow is determined by the intersection of a linear regression to the attenuation curve in the vicinity of the plasma frequency to the 0 dB line.

$$f_p = \frac{1}{2\pi}\sqrt{\frac{n_e e^2}{m_e \varepsilon_0}} \qquad (1)$$

By using Eq. 1 the maximum electron density is derived. The obtained results for the electron density n_e are listed in Tab. 3.

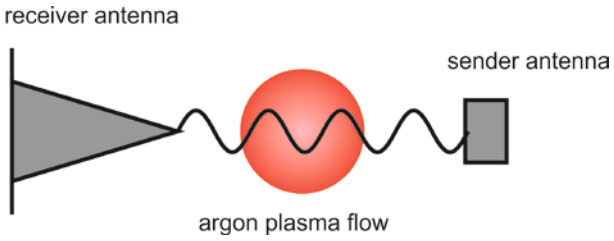

Figure 4. Sketch of MPTS setup.

4. ARGON FLOW AT L2K

For different MHD tests setups different flow states have been defined. A nozzle exit diameter of 200 mm has been chosen for flat plate models, a nozzle exit diameter of 100 mm for stagnation point models. The 200 mm nozzle states have been defined by varying the reservoir pressure, delivering thus a change in the enthalpy and thus the electron density.

The 100 mm nozzle states have been defined by varying both mass flow rate and reservoir pressure to maximize the electron density.

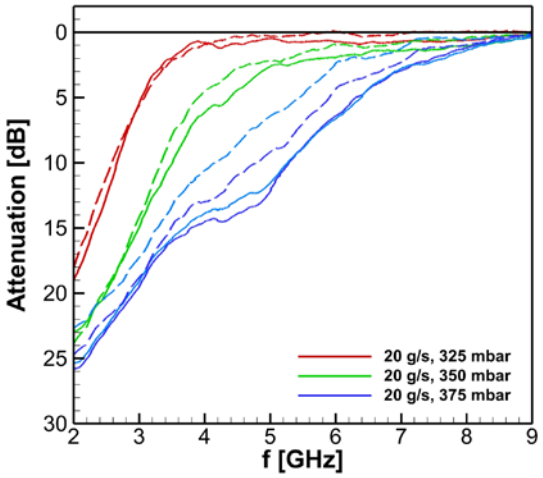

Figure 5. Attenuation spectra measured with the MPTS setup for different 200 mm nozzle exit diameter states.

4.1. Flow parameters

The flow characterization results are listed in Tab. 1 and 2. Here the specific enthalpy and total temperature were computed using the NATA code [14], which is a quasi-one dimensional flow solver including non-equilibrium chemistry. Electron density and flow velocity are MWI data, temperature is derived from DLAS. The pitot pressure profiles for the 200 mm nozzle exit diameter conditions are given in Fig. 6.

4.2. Electron density and electron temperature measurements

The values for the electron density obtained by MWI, MPTS and Langmuir double probe (2L) are compared in Tab. 3. The different values of MPTS refer to spectra from different test runs. The Langmuir probe values have been determined by taking average values over several test runs.

The results of the MWI and MPTS are in good agreement for all states. The values for the Langmuir double probe (2L) are about a factor of 2 higher than those for the other methods. A higher value has to be expected according to the placement of the probe wires behind the bow shock.

Electron density profiles across the flow measured by Langmuir triple probe for the 200 mm nozzle exit diameter states are given in Fig. 7. Steps in the profile are due to the slow current data acquisition. The values

obtained by the triple probe measurements in the range of the values obtained by MWI and MTPS. They have larger uncertainties than the other values due to the spread in the corresponding electron temperatures.

mass flow	**[g/s]**	**20**	**20**	**20**
reservoire pressure	**[hPa]**	**325**	**350**	**375**
specific enthalpy	[MJ/kg]	1.5	1.8	2.0
temperature	[K]	2919	3385	3886
electron density	10^{17} $1/m^3$	1.6	2.7	6.1
velocity	m/s	1723	1850	2150
temperature	K	(-)	(-)	180
Pitot pressure	hPa	4.5	4.9	5.6

Table 1. Flow parameters for 200 mm nozzle exit diameter states.

mass flow	**[g/s]**	**3**	**8**	**20**
reservoir pressure	**[hPa]**	**70**	**160**	**375**
specific enthalpy	[MJ/kg]	3.1	2.4	2.0
temperature	[K]	6010	4532	3886
electron density (MWI)	10^{17} 1/m	8.6	6.8	4.8
velocity (MWI)	m/s	1925	1945	2061
temperature (DLAS)	K	(-)	(-)	360
Pitot pressure	hPa	2.4	4.6	10.0

Table 2. Flow parameters for 100 mm nozzle exit diameter states.

The average results of Langmuir single probe (1L), double probe and triple probe (3L) for the electron temperature are compared in Tab. 4. The given values have been determined by taking average values over several test runs. The data points marked with (-) indicate those conditions for which not enough data was obtained to get a reliable value.

Within the range of uncertainties the values of one method do not differ for the different flow conditions. The single values of single and triple probe are in the same range of about 2500 K to 3500 K whereas the values for the double probe are about a factor of 2 lower in the range of 1500 K. This is a hint that the electron gas is not in thermal equilibrium as the values of the standard evaluation method for Langmuir double probes assumes Maxwell-distributed electron energies.

Further studies have to be done on the reliability of the values and the validity of using the standard analysis routines for determining the electron temperatures and densities from the obtained data.

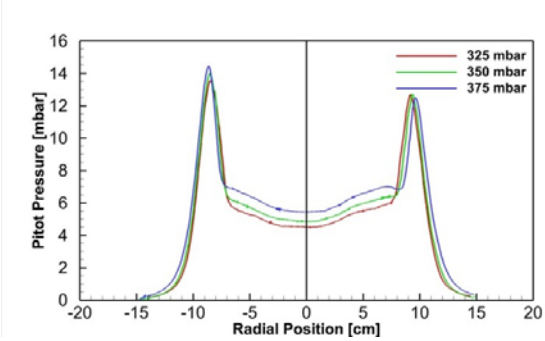

Figure 6. Pitot pressure profiles for the 200 mm nozzle exit diameter states.

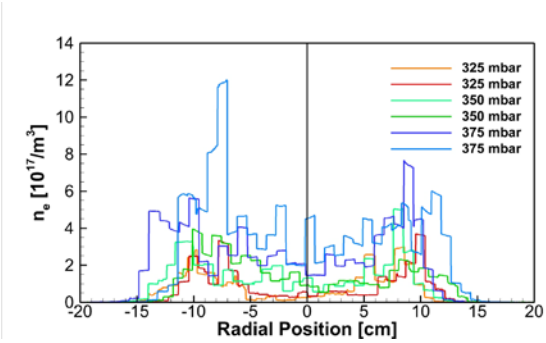

Figure 6. Langmuir triple probe electron density profiles for the 200 mm nozzle exit diameter states.

State (20 g/s)	**MWI**	**MPTS**	**2L**
375 mbar	6.1	6.8	13.3
		7.0	
		5.5	
		6.3	
350 mbar	2.7 ± 0.1	2.6	7.0
		2.2	
325 mbar	1.6 ± 0.2	1.4	3.3
		1.3	

Table 3. Comparison of the electron density values measured by different techniques for 200 mm exit diameter states.

5. MHD EXPERIMENTS

5.1. Experimental Setup

Heat flux mitigation experiments have been set up by using a flat cylindrical stagnation point model of 70 mm diameter made from a quartz cup filled with either an electromagnet (EM) stack of NdFeB permanent magnets (CPM). Both models have an axial alignment of the

magnetic field with a magnetic field strength at the stagnation point of 0.54 T (CPM) resp. 0.48 T (EM). Reference tests for the CPM without magnetic field are executed using a model with a core of demagnetized permanent magnets.

State (20 g/s)	1L	2L	3L
375 mbar	3266	1492	2405
350 mbar	2884	1401	(-)
325 mbar	(-)	1502	(-)

Table 4. Comparison of the electron temperature values measured by different Langmuir probe techniques for 200 mm exit diameter states.

VIS cameras are used to monitor the flow field topology, especially to determine the bow shock standoff distance. An IR camera is used to determine the time history of the temperatures of the quartz surface. From the surface temperature data the surface heat flux is determined by a one dimensional thermal conduction model assuming an adiabatic boundary condition at the inner side of the quartz cup. The heat flux determination is based on the temperature increase closely to the first impact of the argon flow on the model surface to avoid long time influences of the arc heater performance.

5.2. Flow Field Topology

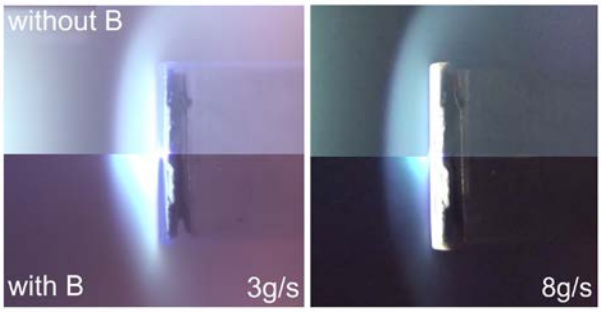

Figure 8. Pictures of flow field topologies for tests with the EM model.

The visibility of the flow field is mostly due to recombination of excited Argon. Excitation is supposed to be mainly due to electron collisions.

The flow field topology of tests with the electromagnet model is depicted in Fig. 8. The results for the 3 g/s state are on the left the ones for the 8 g/s on the right. The upper half shows the results for switched of magnet, the lower half the results for stagnation point magnetic field strength of 0.48 T. The pictures are averaged over a few frames to average out image noise and fluctuations. In both cases a bright sphere in front of the stagnation point appears when the magnetic field is switched on. Also the brightness of the free stream in front of the bow shock is reduced. For the 3 g/s condition without magnetic field the bright sphere extends beyond the bow shock front position for the case without magnetic field.

5.3. Surface Heat Flux Measurements

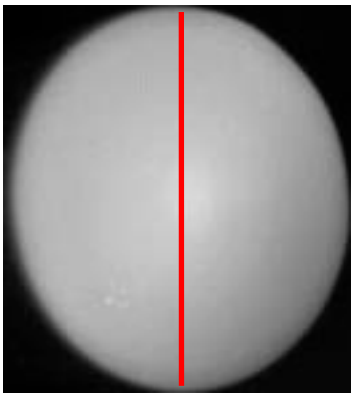

Figure 9. Two dimensional map of the surface heat flux of the CPM for the 3 g/s state.

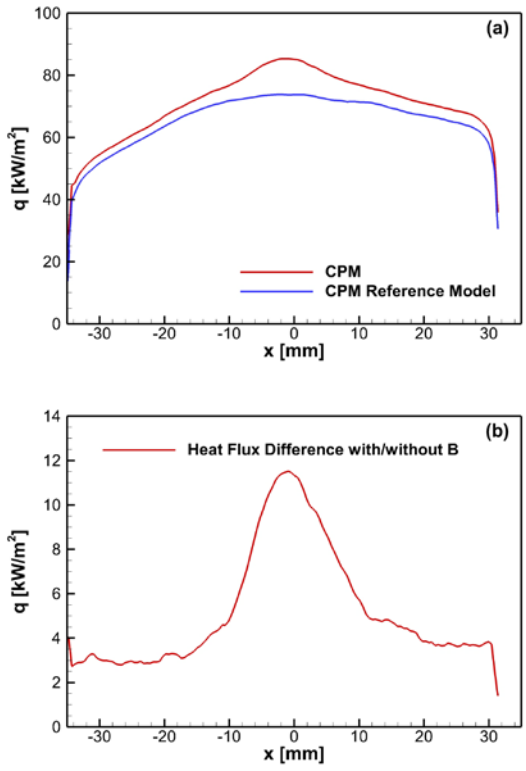

Figure 10.(a) Surface heat flux profiles for CPM and reference tests at 3 g/s.
(b) Difference of the heat flux profiles in (a).

Fig. 9 depicts the two dimensional heat flux map for the CPM for the 3 g/s state. In Fig. 10 (a) the surface heat flux profiles along the vertical line shown in Fig. 9 for CPM tests at 3 g/s is given. The difference of the two heat flux profiles is given in Fig. 10 (b).

The heat flux with magnetic field present shows a peak of 11.5 kW/m^2 at the stagnation point. Off the axis the additional heat flux shows a plateau of 3 to 4 kW/m^2. Measurements with the CPM model at the 8 g/s condition have not been performed due to the higher obtained temperatures which may lead to falsifications due to magnetic field reduction with temperature.

6. CONCLUSIONS

Different Argon flow conditions for two nozzle configurations have been defined for different MHD tests. A thorough characterization of those conditions has been done with multiple methods including spectroscopic methods and different methods to determine the electron density as well as the electron temperature.

Heat flux measurements for the 3 g/s condition at a permanent magnet model showed an increased heat flux for the complete front surface with a distinct heat flux peak at the stagnation point compared to a reference model without MHD.

Flow field topology has been compared for the 3 g/s and 8 g/s conditions for an electromagnet stagnation point model with both magnetic field switched on and off. In case of a present magnetic field a bright sphere in front of the stagnation point appears which in case of the 3 g/s condition extends beyond the bow shock of the corresponding reference case without magnetic field.

7. REFERENCES

1. Resler, E. & Sears, W. (1958). The Prospects for Magneto-Aerodynamics. *Journal of the Aeronautical Sciences* **25**, pp235–245.

2. Kim, M., Keidar, M., & Boyd, I. D. (2008). Effectiveness of an Electromagnetic Mitigation Scheme for Reentry Telemetry Through Plasma. In *AIAA Paper 2008-1394*, presented at the 47th AIAA Aerospace Science Meeting, Reno, NV.

3. Fertig, M., (2015) Investigation of Heatflux Modification by Magnetohydrodynamic Interaction Employing the DLR CFD Code TAU, In *Proc. of the 8th European Symposium on Aerothermo-dynamics for Space Vehicles*. , ESA Publications Division, European Space Agency, Noordwijk, The Netherlands.

4. Gülhan, A., & Esser, B. (2002). Arc-Heated Facilities as a Tool to Study Aerothermodynamic Problems of Reentry Vehicles. Advanced Hypersonic Test Facilities, In *Progress in Astronautics and Aeronautics*, Vol. 198, (Eds. F.K. Lu & D.E. Marren) AIAA, Reston, VA, pp375–403.

5. Gülhan, A., & Esser, B. (2001). A Study on Heat Flux Measurements in High Enthalpy Flows. In *AIAA Paper 2001-3011*, 35th AIAA Thermophysics Conference, Anaheim, CA.

6. Gülhan, A., Esser, B., Koch, U. & Hannemann, K. (2002). Mars Entry Simulation in the Arc Heated Facility L2K. In *Proc of the 4th European Symposium on Aerothermodynamics for Space Vehicles*, ESA-SP-487, ESA Publications Div., Noordwijk, The Netherlands, pp665–772.

7. Koch, U., Steffens, L., Esser, B., Gülhan, A. & Shibusawa, K. (2014), Characterization of Argon flows in the arc heated facility L2K using Diode Laser Absorption spectroscopy on Argon and additional optical diagnostics, In *Proc. of the 6th International Workshop on Radiation of High Temperature Gases in Atmospheric Entry*, St Andrews, UK.

8. Shibusawa, K., Steffens, L., & Koch, U. (2014) Infrared Spectroscopic Measurements of Argon Plasma Flow in Arc Heated Facility L2K, In *Proc. of 46th FDC / ANSS 2014 (Conference CD-ROM)*, JSASS-2014-2014-A, pp1-7.

9. U. Koch, U., Riehmer, J., Esser, B. & Gülhan, A. (2009) Hypersonic Free Stream Characterization in LBK by Laser Induced Fluorescence and Diode Laser Absorption Spectroscopy, In *Proc. of the 3rd International Workshop on Radiation of High Temperature Gases in Atmospheric Entry*, ESA-SP-667, ESA Publications Div., Noordwijk, The Netherlands.

10. Gülhan, A., Esser, B., Koch, U., Siebe, F., Riehmer, J., Giordano, D. & Konigorski, D. (2009). Experimental Verification of Heat-Flux Mitigation by Electromagnetic Fields in Partially-Ionized-Argon Flows. *J. Spacecraft Rockets* **46**(2), pp274-283.

11. Langmuir, I. & Mott-Smith, H.M. (1926) The theory of collectors in gaseous discharges. *Phys. Rev.* **28**. pp727-763.

12. Johnson, E.O. & Maltereca, L. (1950). A Floating Double Probe Method for Measurements in Gas Discharges. *Phys. Rev.* **80(**1).

13. Chen, S.L. & Sekiguchi, T. (1965). Instantaneous Direct-Display System of Plasma Parameters by Means of Triple Probe. *J. Appl. Phys.* **36(**8).

14. Bade, W.L. & Yos, J.M. (1975). The NATA Code, Theory and Analysis, NASA CR-2547.